

RSC Advances



This is an *Accepted Manuscript*, which has been through the Royal Society of Chemistry peer review process and has been accepted for publication.

Accepted Manuscripts are published online shortly after acceptance, before technical editing, formatting and proof reading. Using this free service, authors can make their results available to the community, in citable form, before we publish the edited article. This *Accepted Manuscript* will be replaced by the edited, formatted and paginated article as soon as this is available.

You can find more information about *Accepted Manuscripts* in the [Information for Authors](#).

Please note that technical editing may introduce minor changes to the text and/or graphics, which may alter content. The journal's standard [Terms & Conditions](#) and the [Ethical guidelines](#) still apply. In no event shall the Royal Society of Chemistry be held responsible for any errors or omissions in this *Accepted Manuscript* or any consequences arising from the use of any information it contains.

Novel PARP Inhibitors Sensitize Human Leukemic Cells in an Endogenous PARP Activity Dependent Manner

Mahesh Hegde^a, Kempegowda Mantelingu^a, Hassan A. Swarup^a, Chottanahalli S. Pavankumar^a, Imteyaz Qamar^b, Sathees C. Raghavan^{b*}
and Kanchugarakoppal S. Rangappa^{a*}

^aDepartment of Studies in Chemistry, Manasagangotri, University of Mysore, Mysuru-570006; ^bDepartment of Biochemistry, Indian Institute of Science, Bangalore-560012.

Running title: Identification of a novel PARP inhibitor.

Key words: Double-strand break, DNA damage, Apoptosis, Chemotherapy, PARP inhibitor, Poly (ADP-ribose) polymerase, G2/M arrest

*Corresponding author

Kanchugarakoppal S. Rangappa Ph.: +91-821-2419661; Fax: +91-821-2500846
e-mail: rangappaks@chemistry.uni-mysore.ac.in

Sathees C. Raghavan Ph.: +91 80 2293 2674; Fax: 091 80 2360 0814
e-mail: sathees@biochem.iisc.ernet.in

Abstract

Poly (ADP-ribose) polymerase (PARP) is a critical nuclear enzyme which safeguards genome stability from genotoxic insults and helps in DNA repair. Inhibition of PARP results into sustained DNA damage in cancer cell. PARP inhibitors are known to play an important role in chemotherapy as single agent in many DNA repair pathway deficient tumor cells or in combination with several other chemotherapeutic agents. In the present study, we synthesize and characterize novel pyridazine derivatives, and evaluate their potential to use as PARP inhibitors. Results show that pyridazine derivatives inhibited the PARP1 enzymatic activity at nanomolar range and showed anti-proliferative activity in leukemic cells. Interestingly, human leukemic cell line, Nalm6, in which PARP1 and PARP2 expression as well as intrinsic PARP activity are high, showed significant sensitivity for the novel inhibitors compared to other leukemic cells. Among the inhibitors, P10 showed maximum inhibition of intrinsic PARP activity and inhibited cell proliferation in Nalm6 cells. Besides P10 also showed maximum inhibition against purified PARP1 protein, which was comparable to Olaparib in our assays. Newly synthesized compounds also showed remarkable DNA trapping ability, which is a signature feature of many PARP inhibitors. Importantly, P10 also induced late S and G2/M arrest in Nalm6 cells, indicating accumulation of DNA damage. Therefore, we identify P10 as a potential PARP inhibitor, which can be developed as a chemotherapeutic agent.

Introduction

Poly (ADP-ribose) polymerase (PARP) is an abundant nuclear protein which plays an important role in maintenance of genomic integrity and DNA repair ¹. Among 18 different PARP proteins identified in the family, PARP1 is the major protein to have poly (ADP-ribosyl)ation activity inside the cells as well as major DNA damage sensing potential ². PARP1 protein possesses three domains; N-terminal DNA binding domain containing two main zinc finger motifs which binds to both single- as well as double-strand breaks ³. The central auto modification domain contains a BRCT domain along with certain flanking regions which are hot spots for auto-ADP ribosylation ⁴. The C-terminal catalytic domain where nicotinamide adenine dinucleotide (NAD⁺) binds and acts as a substrate for PARP1 ⁵. Upon DNA damage, PARP1 binds to the damaged site through DNA binding domain and gets activated in several folds to catalyse the transfer of ADP-ribose units from NAD⁺ to itself and other nuclear proteins through its catalytic domain which would otherwise show a basal level activity ⁶.

Recent studies showed that inhibition of DNA repair proteins results in anticancer activity and was shown to enhance the chemotherapeutic strategy ⁷. PARP1 inhibition in homologous recombination deficient cells showed the importance of PARP1 in DNA repair ⁸. Currently, many PARP1 inhibitors are in clinical trial as single agent tools or in combination therapies ⁹.

In present study, we have synthesized novel pyridazine derivatives as potential PARP inhibitors and found that they can inhibit PARP1 enzymatic activity at nanomolar range. Moreover, cytotoxicity studies showed that novel inhibitors induced cytotoxicity in an endogenous PARP activity dependent manner. Importantly, we show the trapping of PARP1 to DNA in presence of novel inhibitors using radiolabelled DNA through EMSA studies. Among the novel pyridazine derivatives, P10 showed maximum activity. Besides, P10 and other inhibitors induced late S and G2/M arrest in human leukemic Nalm6 cell. Therefore, we

identify P10 as a novel PARP inhibitor, which has the potential to be developed as a cancer therapeutic agent.

Materials and Methods

Chemicals and reagents

All the chemicals used in the present study were of analytical grade. NAD⁺ was purchased from SRL (India), CT-DNA is from Sigma (USA) and Olaparib from Selleck Chemicals (USA). Synthetic backbone (**1**) was purchased from Aventura Organica Pharmaceutical Company, Mysuru, India. Antibodies were from Calbiochem, Santa Cruz Biotechnology and Abcam (USA). pET-PARP1 plasmid was a kind gift from Dr. John M. Pascal, Thomas Jefferson University, USA. Oligomeric DNA used in the study were purchased from Sigma-Aldrich, India. Radioisotope-labelled nucleotides were from Board of Radiation and Isotope Technology (BRIT), India.

Chemistry (Synthesis of novel pyridazine derivatives, P9-P13)

An oven-dried Schlenk tube was charged with CuI (0.01 mmol, 1.0 mol %), piperidinone **1** (1.2 mmol) and K₂CO₃ (2.0 mmol, 2 eq), evacuated and back filled with nitrogen and then *N,N*-dimethylethylenediamine (0.1 mmol, 10 mol %), toluene (10 vol) and **2a-2e** (1.0 mmol; for P9-13, respectively) were added under nitrogen. The Schlenk tube was sealed with a Teflon valve and the reaction mixture was stirred at 120 °C for 24 h. The reaction was monitored by TLC. After the completion of reaction, reaction mixture was cooled to room temperature and the resulting suspension was passed through celite bed and washed with ethyl acetate, the solvent was then removed under reduced pressure and obtained residue was purified by silica gel chromatography.

6-(3-(1-(4-chloro-3-fluorophenyl)-2-methyl-6-oxopiperidine-4-carbonyl)-4-fluorobenzyl)-4,5-dimethylpyridazin-3(2H)-one: (P9)

Yield 46%, ^1H NMR (400 MHz, CDCl_3) δ : 11.91 (br s, 1H), 7.75–7.72 (m, 1H), 7.44 (d, $J=6.4$ Hz, 1H), 7.30–7.23 (m, 2H), 7.19–7.12 (m, 2H), 4.33–4.28 (m, 1H), 3.98 (s, 2H), 3.60–3.50 (m, 2H), 3.49–3.41 (m, 1H), 2.61–2.51 (m, 1H), 2.49–2.43 (m, 1H), 2.05 (s, 3H), 1.95 (s, 3H), 1.27 (d, $J=6.4$ Hz, 3H); ^{13}C NMR (100 MHz, CDCl_3) δ : 196.3, 168.7, 163.2, 162.6, 159.7, 155.6, 141.3, 136.5, 135.1, 132.9, 131.6, 130.7, 130.6, 125.9, 122.3, 116.3, 115.9, 113.6, 57.3, 37.3, 35.9, 28.9, 27.3, 16.9, 9.2, 8.3; MS (ES) m/z ($M+1$) = 500.2; Anal. Cald for $\text{C}_{26}\text{H}_{24}\text{ClF}_2\text{N}_3\text{O}_3$: C, 62.46; H, 4.84; N, 8.41; found C, 62.49; H, 4.87; N, 8.46.

6-(3-(1-cyclobutyl-2-methyl-6-oxopiperidine-4-carbonyl)-4-fluorobenzyl)-4,5-dimethylpyridazin-3(2H)-one: (P10)

Yield 48%, ^1H NMR (400 MHz, CDCl_3) δ : 11.85 (br s, 1H), 7.71–7.47 (m, 1H), 7.44–7.39 (m, 1H), 7.27–7.19 (m, 1H), 5.21–5.13 (m, 1H), 4.47–4.42 (m, 1H), 3.98 (s, 2H), 3.65–3.53 (m, 2H), 3.48–3.42 (m, 1H), 2.59–2.55 (m, 2H), 2.50–2.43 (m, 2H), 2.36–2.30 (m, 2H), 2.05 (s, 3H), 2.03 (s, 3H), 1.86–1.75 (m, 2H), 1.17 (d, $J=6.0$ Hz, 3H); ^{13}C NMR (100 MHz, $\text{DMSO}-d_6$) δ : 197.3, 168.3, 162.3, 159.2, 155.6, 137.5, 135.0, 133.6, 132.9, 130.9, 125.6, 115.5, 65.8, 52.4, 43.7, 37.8, 29.6, 27.3, 26.4, 15.6, 15.5, 9.2, 8.8; MS (ES) m/z ($M+1$) = 426.3; Anal. Cald for $\text{C}_{24}\text{H}_{28}\text{FN}_3\text{O}_3$: C, 67.75; H, 6.63; N, 9.88; found C, 67.79; H, 6.66; N, 9.86.

Synthesis of 6-(3-(1-(3,5-difluorophenyl)-2-methyl-6-oxopiperidine-4-carbonyl)-4-fluorobenzyl)-4,5-dimethylpyridazin-3(2H)-one: (P11)

Yield 41%, ^1H NMR (400 MHz, CDCl_3) δ : 11.85 (br s, 1H), 7.73–7.63 (m, 1H), 7.47–7.39 (m, 1H), 7.29–7.11 (m, 2H), 7.14–7.06 (m, 2H), 4.33–4.28 (m, 1H), 3.98 (s, 2H), 3.62–3.51 (m, 2H), 3.48–3.42 (m, 1H), 2.59–2.55 (m, 1H), 2.49–2.44 (m, 1H), 2.03 (s, 3H), 1.99 (s, 3H), 1.21 (d, $J=6.0$ Hz, 3H); ^{13}C NMR (100 MHz, CDCl_3) δ : 190.3, 168.8, 162.3, 159.2, 157.8, 157.4, 155.6, 144.9, 137.5, 135.0, 133.6, 132.9, 130.8, 125.5, 115.3, 105.9, 105.7, 100.2, 57.5, 43.4, 37.0, 35.9, 27.1, 16.8, 9.2, 8.8; MS (ES) m/z ($M+1$) = 484.6; Anal. Cald for $\text{C}_{26}\text{H}_{24}\text{F}_3\text{N}_3\text{O}_3$: C, 64.59; H, 5.00; N, 8.69; found C, 64.54; H, 5.06; N, 8.64.

4-(4-(5-((4,5-dimethyl-6-oxo-1,6-dihydropyridazin-3-yl)methyl)-2-fluorobenzoyl)-2-methyl-6-oxopiperidin-1-yl)-2-fluorobenzonitrile: (P12)

Yield 45%, ¹H NMR (400 MHz, CDCl₃) δ: 11.85 (br s, 1H), 7.73–7.63 (m, 1H), 7.47 (d, *J* = 6.4 Hz, 1H), 7.31–7.23 (m, 2H), 7.21–7.16 (m, 2H), 4.33–4.28 (m, 1H), 3.98 (s, 2H), 3.62–3.51 (m, 2H), 3.48–3.42 (m, 1H), 2.59–2.53 (m, 1H), 2.48–2.41 (m, 1H), 2.00 (s, 3H), 1.98 (s, 3H), 1.20 (d, *J* = 6.4 Hz, 3H); ¹³C NMR (100 MHz, CDCl₃) δ: 195.8, 168.3, 162.3, 160.6, 159.2, 155.6, 147.6, 137.5, 135.0, 134.3, 133.7, 132.9, 130.6, 125.5, 121.3, 117.9, 115.3, 110.8, 108.1, 57.0, 43.4, 37.1, 35.8, 27.2, 16.4, 9.2, 8.8; MS (ES) *m/z* (*M*+1) = 491.2; Anal. Cald for C₂₇H₂₄F₂N₄O₃: C, 66.11; H, 4.93; N, 11.42; found C, 66.14; H, 4.96; N, 11.47.

6-(3-(1-(3-chlorophenyl)-2-methyl-6-oxopiperidine-4-carbonyl)-4-fluorobenzyl)-4,5-dimethylpyridazin-3(2*H*)-one: (P13)

Yield 51 %, ¹H NMR (400 MHz, CDCl₃) δ: 11.79 (br s, 1H), 7.37–7.34 (m, 2H), 7.28–7.22 (m, 2H), 7.18–6.99 (m, 3H), 4.33–4.25 (m, 1H), 3.98 (s, 2H), 3.62–3.51 (m, 2H), 3.48–3.42 (m, 1H), 2.59–2.55 (m, 1H), 2.49–2.44 (m, 1H), 2.03 (s, 3H), 2.01 (s, 3H), 1.14 (d, *J* = 6.4 Hz, 3H); ¹³C NMR (100 MHz, CDCl₃) δ: 195.6, 168.9, 162.3, 159.2, 155.6, 143.1, 137.6, 135.8, 135.2, 135.1, 134.6, 133.9, 132.0, 130.6, 130.3, 127.9, 125.8, 115.3, 43.4, 37.0, 27.1, 25.8, 16.5, 12.9, 9.2, 8.9; MS (ES) *m/z* (*M*+1) = 482.4; Anal. Cald for C₂₆H₂₅ClFN₃O₃: C, 64.80; H, 5.23; N, 8.72; found C, 64.84; H, 5.26; N, 8.76.

Biology

Cell culture

Human cancer cell lines, K562 (Chronic myelogenous leukemia) and Molt4 (acute lymphoblastic leukemia) cells were purchased from National Centre for Cell Science, Pune, India. Nalm6 (B-cell leukemia) and REH (B-cell leukemia) were kind gift from Dr. M.R. Lieber, USA. Cells were cultured in RPMI1640 (Sera Lab, UK) containing 10% FBS (Gibco BRL, USA), 100 U of Penicillin G/ml and 100 µg of streptomycin/ml (Sigma–Aldrich, USA) at 37°C in a humidified atmosphere containing 5% CO₂.

Preparation of cell-free extracts

To test the PARP enzymatic activity inside the cells, cell-free extracts (CFE) were prepared from K562, Molt4, Nalm6 and REH cells. CFE were made from cells as described before¹⁰. Briefly, approximately 2×10^7 cells were washed with phosphate buffered saline, supernatant was carefully removed and re-suspended in 100 μ l of hypotonic lysis buffer containing 10 mM Tris (pH 8.0), 1 mM EDTA and 5 mM DTT followed by 20 min incubation in ice. Cells were homogenized in presence of protease inhibitor (phenylmethylsulfonyl fluoride, 0.01 M; aprotinin, 1 μ g/ml; pepstatin, 1 μ g/ml; leupeptin, 1 μ g/ml) and further incubated on ice for 20 min. 50 μ l of hypertonic solution was added containing 50 mM Tris (pH 7.5), 1 M KCl, 2 mM EDTA and 2 mM DTT and further homogenized on ice. Resulted cell lysate was centrifuged for 3 h at 42 000 r.p.m. at 4°C in a Beckman TLA-100 Rotor (Beckman, Palo Alto, CA, USA). The supernatant was carefully taken out and dialyzed overnight against dialysis buffer containing 20 mM Tris (pH 8.0), 0.1 M KOAc, 20% glycerol, 0.5 mM EDTA and 1 mM DTT, protein amount was estimated using Bradford reagent; snap frozen and stored at -80° C until further use.

PARP expression and activity check in cancer cells

PARP activity inside cells was tested using cell-free extracts as described for PARP1 enzymatic activity assay. Briefly, cell-free extracts (0, 0.01, 0.1, 1, 2, 5, 10 and 20 μ g) were incubated with the reaction buffer containing 1 μ M NAD^+ , 20 μ M activated calf thymus DNA, 50 mM Tris (pH 8.0) and 2 mM MgCl_2 in a reaction volume of 20 μ l for 20 min. Unutilized NAD^+ was measured using fluorescence measurements and plotted (n=6).

Further, to check the expression of PARP1 and PARP2 in K562, Molt4, Nalm6 and REH cells, 30 μ g of cell-free extract was subjected for the western blotting assay using specific antibodies (see also Western blotting in materials method). PARP1 and PARP2 expression was quantified in Multi Gauge V3.0 software and presented as arbitrary unit in bar diagram (n=2)¹¹.

Purification of full length human PARP1 protein

Full length human PARP1 protein was purified as described previously with minor changes¹². pET-PARP1 expressing full length human PARP1 protein was expressed in *Escherichia coli* strain Rosetta (DE3) pLysS. 10 ml of primary culture was inoculated in one litre of LB media containing 50 mg/mL kanamycin and 35 mg/mL chloramphenicol and was grown until O.D (OD₆₀₀) reached to 0.4-0.6. ZnSO₄ (100 mM) was then added to the culture and was grown further till O.D reached to 0.8-1. PARP1 protein was induced with 0.2 mM of IPTG and additionally grown at 16°C for 16 h. Resulting culture was pelleted and suspended in resuspension buffer (10 ml) containing 25 mM HEPES (pH 8.0), 500 mM NaCl, 2 mM beta-mercaptoethanol, 0.1% NP-40 and 1 mM PMSF, sonicated and subjected to centrifugation (14,000 r.p.m., 20 min at 4°C). Clear lysate was passed through the pre-charged Ni-NTA column and washed the column with five volumes of low salt buffer (25 mM HEPES (pH 8.0), 500 mM NaCl, 2 mM beta-mercaptoethanol and 20 mM imidazole) and five volumes of high salt buffer (25 mM HEPES pH 8.0, 1000 mM NaCl, 2 mM beta-mercaptoethanol and 20 mM imidazole) followed by another round of five volumes of low salt buffer. PARP1 protein was eluted in elution buffer containing 25 mM HEPES (pH 8.0), 500 mM NaCl, 2 mM beta-mercaptoethanol and 400 mM imidazole.

PARP1 protein was further purified using phospho-cellulose (Whatman P11) ion exchange chromatography. Briefly, Ni-NTA elutes were mixed with equal volume of no salt buffer (50 mM Tris (pH 7.2), 1 mM EDTA and 2 mM beta-mercaptoethanol) and loaded on to phospho-cellulose column, washed the column with five volume of Buffer A containing 50 mM Tris (pH 7.2), 1 mM EDTA, 2 mM beta-mercaptoethanol and 250 mM NaCl. PARP1 protein was eluted at different concentrations of NaCl in Buffer A and fractions with PARP1 protein were dialysed against 20 mM Tris (pH 8.0), 100 mM NaCl, 1 mM DTT and 25% glycerol for overnight. Dialysed fractions were snap frozen and stored in -80° C. Purity and identity of the PARP1 was assessed by SDS-PAGE followed by Coomassie Brilliant Blue

(CBB) staining and western blotting was performed to confirm the identity of the protein using anti PARP1.

PARP1 enzymatic assays

The newly synthesized PARP inhibitor compounds (P9-13 and Olaparib) were tested for their ability to inhibit PARP activity using purified human full length PARP1 protein as described previously with minor changes¹³. Briefly, different concentrations of compounds (0, 0.5, 1, 5, 10, 25, 50 and 100 nM) were added to the reaction buffer (20 μ l reaction volume) containing 1 μ M NAD⁺, 20 μ M activated calf thymus DNA, 50 mM Tris (pH 8.0) and 2 mM MgCl₂. Reaction was initiated by adding purified PARP1 protein (50 nM) and incubated at room temperature for 20 min. Further, 10 μ l each of 2 M KOH and 20% acetophenone was added and incubated at 4° C (for 10 min). 45 μ l of 88% formic acid was added to the reaction and heated the samples (10 min at 105°C). Samples were cooled and fluorescence measurement for unutilized NAD⁺ was carried out at excitation range of 360 nm and emission range of 445 nm. Reaction sample with only NAD⁺ (no PARP1 protein) was considered as 100%, without NAD⁺ was considered as 0% and compound inhibitory values were converted into percentage and plotted as a sigmoidal curve in GraphPad prism software. IC50 value were determined by log (inhibitor) v/s normalized response variable slope and presented with standard error mean (n=6).

Similarly, inhibition of intrinsic PARP activity in Nalm6 cell extract was carried out using different concentration of compounds (0, 0.1, 0.5, 1, 5, 10, 25, 50 and 100 nM, 4 μ g extract) and followed the similar procedure as mentioned above.

Cytotoxicity studies

The cytotoxic ability of the newly synthesized PARP inhibitors were tested in leukemic cells using MTT assay as described previously¹⁴. Briefly, 50 000 cells/ml were seeded in 24 well plates and treated with different concentration of compounds (for P9 to P13 and Olaparib, 0, 1, 5, 25 and 125 μ M) for 48 and 72 h and cytotoxicity was tested using

MTT assay. For MTT assay, 100 μ l cell suspension was pipetted into the 96 well plate in duplicates, 10 μ l of 5 mg/ml MTT was added and incubated for 2-4 h till the blue colour of formazan crystals appeared. Formazan crystals were solubilized in 67 μ l of solution containing 10% SDS and 50% DMF (60 min at 37 $^{\circ}$ C) and readings were acquired at 570 nm using BioRad iMARK (USA) plate reader. DMSO treated cells were used as vehicle control and considered as 100% cell proliferation. Reading acquired from treated samples was converted into percentage with respect to control and presented as bar diagram. Experiments were repeated minimum two times and data is presented. GI50 values were determined using GraphPad software prism 5.1 and presented.

Oligomers and preparation of nicked DNA substrates

In present study MS68, MS69 and MS70 oligomers were used to make nicked DNA substrate DNA (MS68, 5'-ATCCGTTGAAGCCTGCTT-3'; MS69, 5'-TGACATACTAACTT-GAGCGAAACGG-3' and MS70, 5'-CCGTTTCGCTCAAGTTAGTATGTCAAAGCAGGCTT-CAACGGAT-3', where MS68 and 69 were complementary to MS70 and a nick will be generated upon annealing).

Oligomers were gel purified as described earlier¹⁵, briefly oligomers were suspended in TE buffer and subjected to denaturing polyacrylamide gel electrophoresis (15-18%) and gel purified. The 5' end-labelling of gel purified oligomer was carried out using [γ -³²P] ATP with the help of T4 polynucleotide Kinase and the labelled oligomer was purified using Sephadex G-25 column as described previously and stored at -20 $^{\circ}$ C until further use¹⁶. In order to prepare the nicked DNA substrate, radiolabelled MS68 was slow annealed to cold MS69 and MS70 oligomers in presence of 100 mM NaCl and 1 mM EDTA and annealing was confirmed on a gel.

Electrophoretic mobility shift assay (EMSA) of nicked DNA along with purified human PARP1

EMSA studies were carried out as described previously with modifications¹⁷. Briefly, 5 nM of radiolabelled nicked DNA substrate was incubated with different concentrations of purified human PARP1 protein (0, 5, 10, 20, 50 and 100 nM) in a buffer containing 50 mM Tris (pH 8.0) and 2 mM MgCl₂ for 20 min at room temperature. Subsequently, reaction mixture was resolved on a native PAGE (4%, 100 Volts, 8 h), gels were dried, and signal was detected using PhosphorImager (GE, Pittsburgh, USA). Unbound substrate was quantified using Multi Gauge V3.0 as described before and presented in bar diagram (n=3).

To check the NAD⁺ concentration which is needed to release the nicked DNA substrate from PARP1, EMSA studies were carried out in presence of different concentrations of NAD⁺ (0, 0.1, 1, 10, 100 and 1000 μM). Briefly, 5 nM of radiolabelled nicked DNA substrate was incubated with 20 nM of PARP1 in presence of NAD⁺ in a buffer containing 50 mM Tris (pH 8.0) and 2 mM MgCl₂ for 20 min at room temperature and resolved on native PAGE. Substrates which are bound to PARP1 were quantified using Multi Gauge V3.0 as described before and presented in bar diagram (n=3).

Biochemical assay to assess the trapping of PARP1 in presence of inhibitors

The trapping of PARP1 to the DNA by inhibitors was assessed through the EMSA experiments. Briefly, different concentration of the inhibitors (P9-13 and Olaparib; 0, 0.2, 1 and 5 μM) were mixed with 5 nM radiolabelled nicked DNA substrate, 1 mM NAD⁺ in a buffer containing 50 mM Tris (pH 8.0) and 2 mM MgCl₂, reaction was started by adding 20 nM purified PARP1 protein, reaction mixture was kept at room temperature for 20 min and resolved in native PAGE. DMSO treated samples were taken as control. PARP1 bound substrates were quantified using Multi Gauge V3.0 as described before and presented in bar diagram with minimum three experimental repeats.

Cell cycle analysis

Effect of newly synthesized PARP inhibitors (P9, P10 and P13) on cell cycle progression was tested in Nalm6 cells (10 μM at 12, 24 and 48 h) as described before¹⁸.

Following treatment, cells were harvested, washed with phosphate buffered saline, fixed with 80% chilled ethanol and stored at -20°C ¹⁹, processed for FACS analysis (BD FACSVerse™) after staining with propidium iodide (10 $\mu\text{g}/\text{ml}$). Minimum 10,000 cells were acquired and analysed in Flowing software (version 2.5). Experiments were repeated a minimum of three times and presented as histogram, % of cells in different phases of cell cycle are presented as bar diagram with error bars.

Western blotting analysis

Western blotting analysis was carried out as described earlier²⁰. Briefly, for detection of PARP1 and PARP2 expression, K562, Molt4, Nalm6 and REH cell extract was prepared and subjected to western blotting analysis. Protein amount was measured using Bradford reagent and initial equalization was assessed by using SDS PAGE followed by CBB staining. Approximately 30 μg protein was resolved on a SDS-PAGE (12%), transferred to PVDF membrane (Millipore, USA) and probed with respective primary, biotinylated secondary and streptavidin HRP antibodies. Primary antibodies, PARP1, PARP2 and Actin were used. Membranes were developed using chemiluminescent reagents (Millipore, USA) and images were acquired using gel documentation system (LAS 3000, Fuji, Japan). Ponceau staining was carried out to assess the equal loading of the proteins and experiments were repeated minimum two times.

Statistical analysis

The error bars were expressed as mean \pm SEM. In all the cases statistical analysis was performed using One-way ANOVA followed by Dunnett test and significance was calculated after comparing each value with respective controls using GraphPad software prism 5.1. The values were considered as statistically significant, if the p-value was equal to or less than 0.05 (0.05*, 0.005**, 0.0005***).

Results

Synthesis of novel pyridazine derivatives

Pyridazine derivatives were synthesized as a novel group of heterocyclic compounds and the target molecules were synthesized according to N-arylation method ²¹ using the initial backbone 6-(4-fluoro-3-(2-methyl-6-oxopiperidine-4-carbonyl)benzyl)-4,5-dimethylpyridazin-3(2H)-one, 4,5-dimethylpyridazin-3(2H)-one (1). Copper and N,N-dimethylethylene diamine catalysed N-arylation of amides with arylhalides and cyclobutyl halide was shown to proceed efficiently with combination of K₂CO₃ as a base, and toluene as solvent led to targeted molecules with average yields 41-51% (Fig. 1A and B). Resulting products were purified by silica gel column chromatography and characterized by Mass, ¹H NMR and ¹³C NMR spectroscopy (Suppl. Fig. 1a-j).

Among different leukemic cells, Nalm6 shows higher intrinsic PARP activity

We have used different leukemic cells, K562 (Chronic myelogenous leukemia), Molt4 (acute lymphoblastic leukemia), Nalm6 (B-cell leukemia) and REH (B-cell leukemia) cells for evaluating level of PARP1 and PARP2 through western blotting analysis. Results showed higher expression of PARP1 and PARP2 in Nalm6 cells, among all the leukemic cells tested (Fig. 2A and B). In order to test the intrinsic PARP activity of the leukemic cell lines, cell free extracts prepared from K562, Molt4, Nalm6 and REH cells (using non denaturing method) were incubated with activated calf thymus DNA and NAD⁺. Following incubation with different concentrations of cell-free extracts, unused levels of NAD⁺ were determined using chemical reaction and the fluorescence measurement as described previously ¹³. Interestingly, Nalm6 exhibited highest PARP activity where 1 µg of extract showed significant utilization of NAD⁺ (Fig. 2C). In contrast, K562, Molt4 and REH, where PARP expression was low, showed reduced utilization of NAD⁺ (Fig. 2C). Hence, these results provide a direct correlation between expression of PARP and usage of NAD⁺, which is an indicator of PARP activity.

Ability of the novel pyridazine derivatives in interfering with intrinsic PARP activity was tested using Nalm6 cell extracts by incubating it with increasing concentrations of the inhibitors (0, 0.1, 0.5, 1, 5, 10, 25, 50 and 100 nM). Interestingly, we observed that all the novel pyridazine compounds inhibited NAD^+ utilization in Nalm6 cell extracts, efficiently (Fig. 2D). Olaparib served as the positive control for the assay. Among the derivatives, P10 showed best IC_{50} (~2.77 nM), while others showed lower IC_{50} values (Fig. 2E). Therefore, novel pyridazine derivatives possess PARP inhibition ability and among the molecules tested, P10 showed the highest potential in inhibiting intrinsic PARP activity.

Novel pyridazine derivatives inhibits PARP1 enzymatic activity

Pyridazine derivatives (P9 to P13) were tested for their ability to inhibit PARP1 enzymatic activity using full length human PARP1 protein and NAD^+ (1 μM) in presence of activated calf thymus DNA. It is established that in presence of broken DNA ends, PARP1 enzymatic activity gets highly activated through its double zinc finger DNA-binding domain and modifies itself through extensive polymers of ADP-ribose (PAR) from donor NAD^+ molecules^{2c}. Full length human PARP1 was purified after over expression in bacteria and identity was confirmed using anti PARP1 antibody by performing western blotting (Fig. 3A, B). In order to evaluate the efficacy of pyridazine derivatives, purified PARP1, NAD^+ , activated calf thymus DNA were incubated in MgCl_2 containing buffer along with different concentration of inhibitors and NAD^+ utilization was determined as described above. Olaparib was used as a positive control for the assay. Interestingly, we found that among the compounds tested, P10 showed maximum inhibition against purified PARP1 enzymatic activity (IC_{50} ~ 7.4 nM), which was comparable to that of Olaparib (~7.8 nM) (Fig. 3C, D). Other derivatives such as P13 and P9 also exhibited higher levels of PARP inhibition (Fig. 3C, D). Therefore, our results suggest that newly synthesized pyridazine derivatives are able to inhibit PARP1 enzymatic activity, and among the molecules P10 showed best activity.

Novel pyridazine derivatives inhibit proliferation of leukemic cells in a PARP dependent manner

We checked the anti-proliferative activity of the newly synthesized compounds on leukemic cells, K562, Molt4, Nalm6 and REH. Cells were incubated with increasing concentration of inhibitors (1, 5, 25 and 125 μM for 48 and 72 h) and impact on cell proliferation was evaluated using MTT assay. Interestingly, we observed that all compounds affected cell proliferation significantly in Nalm6 cells, where PARP expression and activity was higher, while other cell lines were less sensitive, which was true in the case of Olaparib as well (Fig. 4). These results suggest that all the derivatives induced cytotoxicity in different leukemic cells in a PARP expression and activity dependent manner. Among the derivatives, P10, P13 and P9 showed maximum sensitivity in Nalm6 cells with a GI50 of 8.8, 10.3 and 12.7 μM , respectively, while other derivatives showed ~ 50 μM (Fig. 4B). Interestingly the GI50 of P10 was in the same range of Olaparib and suggest that it could be considered as an alternative for Olaparib.

Novel pyridazine derivatives induce trapping of PARP1 to DNA

Previous studies suggest that ability of PARP inhibitors to induce anti-proliferative effect is not only dependent on its catalytic inhibition, but also depending on its ability to induce trapping of PARP to DNA²². Therefore, ability of the newly synthesized pyridazine derivatives were tested for their impact on the trapping of purified PARP1 to radiolabelled nicked DNA substrate using electrophoretic mobility shift assay (EMSA). Since PARP1 has affinity towards nicked or gaped DNA substrates²³, we incubated nicked radiolabelled DNA substrate with increasing concentration of purified PARP1 and evaluated subsequent binding (Fig. 5A). Results showed shift in mobility of radiolabelled nicked DNA substrates upon binding to PARP1 (Fig. 5A). A concentration of 20 nM PARP1 was sufficient to induce mobility shift to most of the radiolabelled DNA substrate (Fig. 5A, B) and was used in further assays.

(Poly-ADP) ribosylation by NAD^+ lead to release of bound PARP1 from the DNA ²⁴. We tested whether addition of increasing NAD^+ concentration could result in the release of PARP1 from the radiolabelled nicked DNA. Results showed that a concentration of 1 μM of NAD^+ disturbed the complex formation completely and further increase in the NAD^+ levels did not have any impact (Fig. 5C, D). Trapping of the PARP1 to the nicked DNA substrate was carried out in presence of 1 mM NAD^+ in presence of increasing concentrations of compounds (0.2, 1 and 5 μM) and subjected to EMSA studies (Fig. 5E). Interestingly, we found that P10 and P13 were able trap PARP1 to DNA substrate more strongly than P9, P11 and P12 compounds (Fig. 5E, F). However, Olaparib showed better DNA trapping compared to P10. Therefore, our data suggest that along with the catalytic inhibition, novel pyridazine derivatives, particularly, P10 was able to induce trapping of the PARP1 to DNA *in vitro*. These results imply that although P10 has an equal or better inhibitor activity on PARP enzymatic activity compared to Olaparib, latter showed better DNA trapping ability than former, which may suggest the importance of DNA trapping in inhibition of cell proliferation.

Novel PARP inhibitors induces cell cycle arrest at late S and G2/M phases

Newly synthesized PARP inhibitors P9, P10 and P13 were tested to check whether they affect cell cycle progression. Nalm6 cells were treated with P9, P10 and P13 (10 μM) for 12, 24 and 48 h, harvested, PI stained and subjected to flow cytometric analysis (Fig. 6A). Interestingly, we observed significant increase in late S and G2/M phase cell population when treated with compounds and was prominent at 24 h time point (Fig. 6). This suggests that inhibition of PARP activity in cells could lead to elevated levels of DNA damage and hence cell cycle arrest.

Discussion

PARP inhibitors gained significant attention when they were found to induce 'synthetic lethality' in BRCA2 deficient breast cancer cells^{8a, 8c}, since the cells were unable to undergo repair due to inhibition of enzymatic activity of PARP1 inside the cells. Since then,

several attempts were made to understand the process of PARP inhibition in different cancer cell lines with the background of multiple genetically mutant/absent proteins^{9c, 22}. Among the ongoing clinical trials using PARP inhibitors²⁵, 'Olaparib' has been recently approved for cancer therapy against deleterious germline BRCA-mutated advanced ovarian cancers²⁶.

Newly synthesized pyridazine derivatives were tested for their anticancer activity against various cancers of haematopoietic origin (K562, Molt4, Nalm6 and REH). Interestingly, we observed that 'Nalm6', a human pre B leukemic cell line, possesses both, higher levels of intrinsic PARP activity as well as PARP1 and PARP2 expression among the cancer cell lines tested. Importantly, the same cell line showed maximum sensitivity towards the novel inhibitors with respect to inhibition of intrinsic PARP activity, both in biochemical studies as well as *ex vivo* experiments. Among the inhibitors, P10 showed the maximum inhibitory activity in various assays.

Studies using purified human full length PARP1 showed that all the pyridazine derivatives can indeed target specifically PARP and interfere with its enzymatic activity. However, among the derivatives P10 showed the best inhibition, which was comparable to Olaparib.

The novel scaffold 6-(4-fluoro-3-(2-methyl-6-oxopiperidine-4-carbonyl)benzyl)-4,5-dimethylpyridazin-3(2H)-one, 4,5-dimethylpyridazin-3(2H)-one was designed by envisaging that pyridazine heterocyclic could bind in the nicotinamide pocket and the heterocyclic sandwiched between Tyr-896 and Tyr-907 amino acids, and the lactam of the pyrazinone making three H-bonds to enzyme²⁷. The pendant fluorobenzyl group could then reach down into the adenine binding pocket allowing any substituent to make further binding interactions to improve affinity. Although basic skeleton of our PARP inhibitors, P9-P13 is quite similar to Olaparib, we replaced fused benzene ring by dimethyl groups and incorporated a lactam like carbonyls to improve cellular potency. These modifications provided a series of efficient PARP inhibitors, among which P10 was found to be most potent in both intrinsic and cellular

assays. Nevertheless, all the compounds displayed significant activity against PARP1, presumably due to a large binding pocket at this area of the protein. Substituted cyclocarbonyl ring attached to the lactam like carbonyls showed great impact on the activity. Since, 2-oxopiperazine moiety in previously reported pyridazine PARP1 inhibitors showed potent inhibitory activity, we maintained similar appendage in our inhibitors²⁸. The additional amide functionality could be crucial for binding to the enzymatic site. Besides, it appears that the substituted cyclobutyl group in P10 would have contributed towards its increased antiproliferative activity.

The observed inhibition by novel pyridazine derivatives on intrinsic PARP activity in Nalm6 cell extract showed an IC₅₀ value of 2-4 nM (Fig. 2E). However, when the inhibitory effect was tested against purified PARP1 it showed much higher IC₅₀ values (range of 7-13 nM; Fig. 3D). The observed less inhibitory action on purified PARP1 is puzzling. One of the potential explanations could be the presence of multiple NAD⁺ utilizing enzymes in the cell free extracts. This is very much possible as PARP family alone comprises of 18 different proteins where novel inhibitors might play a role in suppressing the activity of some other proteins which are known to have PARylation activity inside the cells^{2a}. This is also evident in case of Olaparib, which is known to show significant inhibitory activity on PARP2 compared to PARP1. Observed PARP2 expression in Nalm6 cells and higher sensitivity by novel pyridazine inhibitors in Nalm6 suggest the plausible inhibition of PARP2 as well. However, inhibition of PARP1 is important because of its high PARylation activity inside the cell (more than 85%)²⁹.

Ex vivo antiproliferation assays also revealed that among the cell lines tested, the PARP positive Nalm6 cells showed best activity against the novel molecules and Olaparib. Besides, among the molecules, P10 showed maximum antiproliferative activity, which was comparable to that of Olaparib. More importantly, sensitivity of different cell lines to P10 and other molecules can be directly correlated with the intrinsic PARP activity of the cells rather than just expression levels (Fig. 2, 4). This is important based on the previous report that

several leukemic cells show different level of PARP activity despite varying level of its expression³⁰. However, the cumulative inhibitory activity exhibited by the novel inhibitors could be due to their effect on different isoforms of PARP as well and this needs to be investigated further.

Recent studies have shown that along with the ability of catalytic inhibition of PARP1, inhibitors also possess the PARP1 poisoning/trapping ability to DNA³¹ which would be more appropriate method to categorize the PARP inhibitors. In this regard, we observe that P10 and other inhibitors possess DNA trapping ability. Among the molecules reported here, P10 showed highest trapping ability compared to other derivatives; however P10 induced trapping was less compared to Olaparib.

P10 inhibited activity of purified PARP1, which was comparable to Olaparib, however the former showed reduced DNA trapping activity than Olaparib. These intriguing results suggest that the similar cytotoxic activity contributed by P10 and Olaparib is of interest. It is possible that the mechanism of action of the PARP inhibitors could be different inside the cells, as P10 might act predominantly by blocking the PARP enzymatic activity. This can have several implications considering that PARP enzymatic activity is important during SSB repair and recently discovered MMEJ. The cell cycle arrest induced by P10 and other derivatives also suggest the possibility of increased DNA damage within the cells upon treatment in Nalm6 cells. However, further studies are required to delineate these aspects.

Overall, we identify a novel PARP inhibitor in the present study, show the potential of targeting the intrinsic PARP activity for the treatment of cancer cells using PARP inhibitors which could have implications in personalized medicine and cancer therapy.

Acknowledgements

We thank Dr. Mridula Nambiar and other members of SCR laboratory for discussions and comments on the manuscript. We thank NMR and FACS facility at IISc for their help. Pavan Beleyur is acknowledged for reagent. This work was supported by grants from DST

(F.NO.SR/SO/HS-006/2010 (G) Dated 29.08.2011) to KSR and SCR, IISc-DBT partnership programme [DBT/BF/PR/INS/2011-12/IISc] to SCR and DST-Fastrack, New Delhi (grant no. SERB/F/5061/2013-14 dated 31-10-2013) to KM. MH is supported by Junior Research Fellowship from DST-PURSE program and DST (F.NO.SR/SO/HS-006/2010 (G) Dated 29.08.2011). We sincerely thank Dr. Ganesh Nagaraju, Indian Institute of Science, India for providing PARP2 antibody and Dr. John M. Pascal, Thomas Jefferson University, USA for providing pET-PARP1 plasmid.

Conflict of interest

Authors disclose that there is no conflict of interest.

References

1. (a) de Murcia, J. M.; Niedergang, C.; Trucco, C.; Ricoul, M.; Dutrillaux, B.; Mark, M.; Oliver, F. J.; Masson, M.; Dierich, A.; LeMeur, M.; Walztinger, C.; Chambon, P.; de Murcia, G., Requirement of poly(ADP-ribose) polymerase in recovery from DNA damage in mice and in cells. *Proc. Natl. Acad. Sci. U S A.*, **1997**, *94* (14), 7303-7; (b) Chambon, P.; Weill, J. D.; Mandel, P., Nicotinamide mononucleotide activation of new DNA-dependent polyadenylic acid synthesizing nuclear enzyme. *Biochem. Biophys. Res. Commun.*, **1963**, *11*, 39-43; (c) Ame, J. C.; Spelshauer, C.; de Murcia, G., The PARP superfamily. *Bioessays.*, **2004**, *26* (8), 882-93; (d) Huber, A.; Bai, P.; de Murcia, J. M.; de Murcia, G., PARP-1, PARP-2 and ATM in the DNA damage response: functional synergy in mouse development. *DNA Repair*, **2004**, *3* (8-9), 1103-8.
2. (a) Jagtap, P.; Szabo, C., Poly(ADP-ribose) polymerase and the therapeutic effects of its inhibitors. *Nat. Rev. Drug. Discov.*, **2005**, *4* (5), 421-40; (b) Bouchard, V. J.; Rouleau, M.; Poirier, G. G., PARP-1, a determinant of cell survival in response to DNA damage. *Exp. Hematol.*, **2003**, *31* (6), 446-54; (c) D'Amours, D.; Desnoyers, S.; D'Silva, I.; Poirier, G. G., Poly(ADP-ribosyl)ation reactions in the regulation of nuclear functions. *Biochem. J.*, **1999**, *342* (Pt 2), 249-68.
3. d'Adda di Fagagna, F.; Hande, M. P.; Tong, W. M.; Lansdorp, P. M.; Wang, Z. Q.; Jackson, S. P., Functions of poly(ADP-ribose) polymerase in controlling telomere length and chromosomal stability. *Nat. Genet.*, **1999**, *23* (1), 76-80.
4. (a) Altmeyer, M.; Messner, S.; Hassa, P. O.; Fey, M.; Hottiger, M. O., Molecular mechanism of poly(ADP-ribosyl)ation by PARP1 and identification of lysine residues as ADP-ribose acceptor sites. *Nucleic Acids Res.*, **2009**, *37* (11), 3723-38; (b) Tao, Z.; Gao, P.;

Liu, H. W., Identification of the ADP-ribosylation sites in the PARP-1 automodification domain: analysis and implications. *J. Am. Chem. Soc.*, **2009**, *131* (40), 14258-60.

5. Ruf, A.; Mennissier de Murcia, J.; de Murcia, G.; Schulz, G. E., Structure of the catalytic fragment of poly(AD-ribose) polymerase from chicken. *Proc. Natl. Acad. Sci. U S A.*, **1996**, *93* (15), 7481-5.

6. (a) Jeggo, P. A., DNA repair: PARP - another guardian angel? *Curr. Biol.*, **1998**, *8* (2), R49-51; (b) Schreiber, V.; Dantzer, F.; Ame, J. C.; de Murcia, G., Poly(ADP-ribose): novel functions for an old molecule. *Nat. Rev. Mol. Cell. Biol.*, **2006**, *7* (7), 517-28.

7. (a) Srivastava, M.; Nambiar, M.; Sharma, S.; Karki, S. S.; Goldsmith, G.; Hegde, M.; Kumar, S.; Pandey, M.; Singh, R. K.; Ray, P.; Natarajan, R.; Kelkar, M.; De, A.; Choudhary, B.; Raghavan, S. C., An inhibitor of nonhomologous end-joining abrogates double-strand break repair and impedes cancer progression. *Cell*, **2012**, *151* (7), 1474-87; (b) Srivastava, M.; Raghavan, S. C., DNA double-strand break repair inhibitors as cancer therapeutics. *Chem. Biol.*, **2015**, *22* (1), 17-29; (c) Gad, H.; Koolmeister, T.; Jemth, A. S.; Eshtad, S.; Jacques, S. A.; Strom, C. E.; Svensson, L. M.; Schultz, N.; Lundback, T.; Einarsdottir, B. O.; Saleh, A.; Gokturk, C.; Baranczewski, P.; Svensson, R.; Berntsson, R. P.; Gustafsson, R.; Stromberg, K.; Sanjiv, K.; Jacques-Cordonnier, M. C.; Desroses, M.; Gustavsson, A. L.; Olofsson, R.; Johansson, F.; Homan, E. J.; Loseva, O.; Brautigam, L.; Johansson, L.; Hoglund, A.; Hagenkort, A.; Pham, T.; Altun, M.; Gaugaz, F. Z.; Vikingsson, S.; Evers, B.; Henriksson, M.; Vallin, K. S.; Wallner, O. A.; Hammarstrom, L. G.; Wiita, E.; Almlof, I.; Kalderen, C.; Axelsson, H.; Djureinovic, T.; Puigvert, J. C.; Haggblad, M.; Jeppsson, F.; Martens, U.; Lundin, C.; Lundgren, B.; Granelli, I.; Jensen, A. J.; Artursson, P.; Nilsson, J. A.; Stenmark, P.; Scobie, M.; Berglund, U. W.; Helleday, T., MTH1 inhibition eradicates cancer by preventing sanitation of the dNTP pool. *Nature*, **2014**, *508* (7495), 215-21.

8. (a) Bryant, H. E.; Schultz, N.; Thomas, H. D.; Parker, K. M.; Flower, D.; Lopez, E.; Kyle, S.; Meuth, M.; Curtin, N. J.; Helleday, T., Specific killing of BRCA2-deficient tumours with inhibitors of poly(ADP-ribose) polymerase. *Nature*, **2005**, *434* (7035), 913-7; (b) De Lorenzo, S. B.; Patel, A. G.; Hurley, R. M.; Kaufmann, S. H., The Elephant and the Blind Men: Making Sense of PARP Inhibitors in Homologous Recombination Deficient Tumor Cells. *Front. Oncol.*, **2013**, *3*, 228; (c) Farmer, H.; McCabe, N.; Lord, C. J.; Tutt, A. N.; Johnson, D. A.; Richardson, T. B.; Santarosa, M.; Dillon, K. J.; Hickson, I.; Knights, C.; Martin, N. M.; Jackson, S. P.; Smith, G. C.; Ashworth, A., Targeting the DNA repair defect in BRCA mutant cells as a therapeutic strategy. *Nature*, **2005**, *434* (7035), 917-21.

9. (a) Rodon, J.; Iniesta, M. D.; Papadopoulos, K., Development of PARP inhibitors in oncology. *Expert Opin. Investig. Drugs*, **2009**, *18* (1), 31-43; (b) Curtin, N. J.; Szabo, C., Therapeutic applications of PARP inhibitors: anticancer therapy and beyond. *Mol. Aspects*

- Med.*, **2013**, *34* (6), 1217-56; (c) Shen, Y.; Rehman, F. L.; Feng, Y.; Boshuizen, J.; Bajrami, I.; Elliott, R.; Wang, B.; Lord, C. J.; Post, L. E.; Ashworth, A., BMN 673, a novel and highly potent PARP1/2 inhibitor for the treatment of human cancers with DNA repair deficiency. *Clin. Cancer Res.*, **2013**, *19* (18), 5003-15.
10. (a) Sharma, S.; Javadekar, S. M.; Pandey, M.; Srivastava, M.; Kumari, R.; Raghavan, S. C., Homology and enzymatic requirements of microhomology-dependent alternative end joining. *Cell Death Dis.*, **2015**, *6*, e1697; (b) Baumann, P.; West, S. C., DNA end-joining catalyzed by human cell-free extracts. *Proc. Natl. Acad. Sci. U S A.*, **1998**, *95* (24), 14066-70.
11. Kumar, T. S.; Kari, V.; Choudhary, B.; Nambiar, M.; Akila, T. S.; Raghavan, S. C., Anti-apoptotic protein BCL2 down-regulates DNA end joining in cancer cells. *J. Biol. Chem.*, **2010**, *285* (42), 32657-70.
12. (a) Langelier, M. F.; Servent, K. M.; Rogers, E. E.; Pascal, J. M., A third zinc-binding domain of human poly(ADP-ribose) polymerase-1 coordinates DNA-dependent enzyme activation. *J. Biol. Chem.*, **2008**, *283* (7), 4105-14; (b) Langelier, M. F.; Planck, J. L.; Servent, K. M.; Pascal, J. M., Purification of human PARP-1 and PARP-1 domains from *Escherichia coli* for structural and biochemical analysis. *Methods Mol. Biol.*, **2011**, *780*, 209-26.
13. Putt, K. S.; Hergenrother, P. J., An enzymatic assay for poly(ADP-ribose) polymerase-1 (PARP-1) via the chemical quantitation of NAD(+): application to the high-throughput screening of small molecules as potential inhibitors. *Anal. Biochem.*, **2004**, *326* (1), 78-86.
14. (a) Katiyar, A.; Hegde, M.; Kumar, S.; Gopalakrishnan, V.; Bhatelia, K. D.; Ananthaswamy, K.; Ramareddy, S. A.; De Clercq, E.; Choudhary, B.; Schols, D.; Raghavan, S. C.; Karki, S. S., Synthesis and evaluation of the biological activity of N'-[2-oxo-1,2 dihydro-3H-indol-3-ylidene] benzohydrazides as potential anticancer agents. *RSC Adv.* **2015**, *5* (56), 45492-45501; (b) Hegde, M.; Karki, S. S.; Thomas, E.; Kumar, S.; Panjamurthy, K.; Ranganatha, S.R.; Rangappa, K. S.; Choudhary, B.; Raghavan, S. C., Novel levamisole derivative induces extrinsic pathway of apoptosis in cancer cells and inhibits tumor progression in mice. *PLoS One*, **2012**, *7* (9), e43632; (c) Hegde, M.; Sharath Kumar, K. S.; Thomas, E.; Ananda, H.; Raghavan, S. C.; Rangappa, K. S., A novel benzimidazole derivative binds to the DNA minor groove and induces apoptosis in leukemic cells. *RSC Adv.* **2015**, *5* (113), 93194-93208.
15. Nambiar, M.; Srivastava, M.; Gopalakrishnan, V.; Sankaran, S. K.; Raghavan, S. C., G-quadruplex structures formed at the HOX11 breakpoint region contribute to its fragility during t(10;14) translocation in T-cell leukemia. *Mol. Cell. Biol.*, **2013**, *33* (21), 4266-81.

16. (a) Nambiar, M.; Raghavan, S. C., Mechanism of fragility at BCL2 gene minor breakpoint cluster region during t(14;18) chromosomal translocation. *J. Biol. Chem.*, **2012**, *287* (12), 8688-701; (b) Sharma, S.; Choudhary, B.; Raghavan, S. C., Efficiency of nonhomologous DNA end joining varies among somatic tissues, despite similarity in mechanism. *Cell. Mol. Life. Sci.*, **2011**, *68* (4), 661-76.
17. (a) Nishana, M.; Raghavan, S. C., A non-B DNA can replace heptamer of V(D)J recombination when present along with a nonamer: implications in chromosomal translocations and cancer. *Biochem. J.*, **2012**, *448* (1), 115-25; (b) Kumari, R.; Raghavan, S. C., Structure-specific nuclease activity of RAGs is modulated by sequence, length and phase position of flanking double-stranded DNA. *FEBS. J.*, **2015**, *282* (1), 4-18.
18. Srivastava, M.; Hegde, M.; Chiruvella, K. K.; Koroth, J.; Bhattacharya, S.; Choudhary, B.; Raghavan, S. C., Sapodilla plum (*Achras sapota*) induces apoptosis in cancer cell lines and inhibits tumor progression in mice. *Sci. Rep.*, **2014**, *4*, 6147.
19. Kumar, S.; Gopalakrishnan, V.; Hegde, M.; Rana, V.; Dhepe, S. S.; Ramareddy, S. A.; Leoni, A.; Locatelli, A.; Morigi, R.; Rambaldi, M.; Srivastava, M.; Raghavan, S. C.; Karki, S. S., Synthesis and antiproliferative activity of imidazo[2,1-b][1,3,4]thiadiazole derivatives. *Bioorg. Med. Chem. Lett.*, **2014**, *24* (19), 4682-8.
20. Somasagara, R. R.; Hegde, M.; Chiruvella, K. K.; Musini, A.; Choudhary, B.; Raghavan, S. C., Extracts of strawberry fruits induce intrinsic pathway of apoptosis in breast cancer cells and inhibits tumor progression in mice. *PLoS One*, **2012**, *7* (10), e47021.
21. (a) Klapars, A.; Antilla, J. C.; Huang, X.; Buchwald, S. L., A general and efficient copper catalyst for the amidation of aryl halides and the N-arylation of nitrogen heterocycles. *J. Am. Chem. Soc.*, **2001**, *123* (31), 7727-9; (b) Allen, A. J.; Hemrick-Luecke, S.; Sumner, C. R.; Wallace, O. B., Treatment of hot flashes, impulse control disorders and personality change due to a general medical condition, US patent/0015786 A1: **2007**.
22. Murai, J.; Huang, S. Y.; Das, B. B.; Renaud, A.; Zhang, Y.; Doroshov, J. H.; Ji, J.; Takeda, S.; Pommier, Y., Trapping of PARP1 and PARP2 by Clinical PARP Inhibitors. *Cancer Res.*, **2012**, *72* (21), 5588-99.
23. Eustermann, S.; Videler, H.; Yang, J. C.; Cole, P. T.; Gruszka, D.; Veprintsev, D.; Neuhaus, D., The DNA-binding domain of human PARP-1 interacts with DNA single-strand breaks as a monomer through its second zinc finger. *J. Mol. Biol.*, **2011**, *407* (1), 149-70.
24. Steffen, J. D.; Tholey, R. M.; Langelier, M. F.; Planck, J. L.; Schiewer, M. J.; Lal, S.; Bildzukewicz, N. A.; Yeo, C. J.; Knudsen, K. E.; Brody, J. R.; Pascal, J. M., Targeting PARP-1 allosteric regulation offers therapeutic potential against cancer. *Cancer Res.*, **2014**, *74* (1), 31-7.

25. (a) Ratnam, K.; Low, J. A., Current development of clinical inhibitors of poly(ADP-ribose) polymerase in oncology. *Clin. Cancer Res.*, **2007**, *13* (5), 1383-8; (b) Rouleau, M.; Patel, A.; Hendzel, M. J.; Kaufmann, S. H.; Poirier, G. G., PARP inhibition: PARP1 and beyond. *Nat. Rev. Cancer*, **2010**, *10* (4), 293-301.
26. Kim, G.; Ison, G.; McKee, A. E.; Zhang, H.; Tang, S.; Gwise, T.; Sridhara, R.; Lee, E.; Tzou, A.; Philip, R.; Chiu, H. J.; Ricks, T. K.; Palmby, T.; Russell, A. M.; Ladouceur, G.; Pfuma, E.; Li, H.; Zhao, L.; Liu, Q.; Venugopal, R.; Ibrahim, A.; Pazdur, R., FDA Approval Summary: Olaparib Monotherapy in Patients with Deleterious Germline BRCA-Mutated Advanced Ovarian Cancer Treated with Three or More Lines of Chemotherapy. *Clin. Cancer Res.*, **2015**.
27. Pescatore, G.; Branca, D.; Fiore, F.; Kinzel, O.; Bufi, L. L.; Muraglia, E.; Orvieto, F.; Rowley, M.; Toniatti, C.; Torrisi, C.; Jones, P., Identification and SAR of novel pyrrolo[1,2-a]pyrazin-1(2H)-one derivatives as inhibitors of poly(ADP-ribose) polymerase-1 (PARP-1). *Bioorg. Med. Chem. Lett.*, **2010**, *20* (3), 1094-9.
28. (a) Branca, D.; Dessole, G.; Ferrigno, F.; Jones, P.; Kinzel, O.; Lillini, S.; Muraglia, E.; Pescatore, G.; Schultz-Fademrecht, C., Pyridazinone derivatives as parp inhibitors. US patent/0261709 A1 **2010**; (b) Jones, P.; Kinzel, O.; Pescatore, G.; Bufi, L. L.; Schultz-Fademrecht, C.; Ferrigno, F., Pyridinone and pyridazinone derivatives as inhibitors of poly(adp-ribose) polymerase (PARP). US patent/0176765 A1 **2009**.
29. Dal Piaz, F.; Ferro, P.; Vassallo, A.; Vasaturo, M.; Forte, G.; Chini, M. G.; Bifulco, G.; Tosco, A.; De Tommasi, N., Identification and mechanism of action analysis of the new PARP-1 inhibitor 2"-hydroxygenkwanol A. *Biochim. Biophys. Acta.*, **2015** *1850* (9), 1806-14.
30. Zaremba, T.; Ketzner, P.; Cole, M.; Coulthard, S.; Plummer, E. R.; Curtin, N. J., Poly(ADP-ribose) polymerase-1 polymorphisms, expression and activity in selected human tumour cell lines. *Br. J. Cancer*, **2009**, *101* (2), 256-62.
31. Murai, J.; Huang, S. Y.; Renaud, A.; Zhang, Y.; Ji, J.; Takeda, S.; Morris, J.; Teicher, B.; Doroshow, J. H.; Pommier, Y., Stereospecific PARP trapping by BMN 673 and comparison with olaparib and rucaparib. *Mol. Cancer Ther.*, **2014**, *13* (2), 433-43.

Figure Legends

Figure 1. Synthesis of novel pyridazine derivatives. A. Scheme for the synthesis of novel pyridazine derivatives P9 to P13. **B.** Table showing name of the compounds with their respective functional R group (2a to 2e).

Figure 2. Evaluation of different novel pyridazine derivatives on PARP activity present in different leukemic cells. **A.** Western blotting showing expression of PARP1 and PARP2 in leukemic cell lines, K562, Molt4, Nalm6 and REH. Cell-free extracts of different leukemic cells were subjected to western blotting analysis and Actin was used as a loading control. Ponceau stained blot was also shown for equal loading of protein. **B.** Quantification of PARP1 and PARP2 expression levels based on western blotting profile presented as a bar diagram (n=2). **C.** PARP activity inside the cells was measured using cell-free extracts prepared from K562, Molt4, Nalm6 and REH cells (0, 0.01, 0.1, 1, 2, 5, 10 and 20 μg). Unutilized NAD^+ was measured using fluorimetric methods and plotted as percentage unutilized NAD^+ verses log concentration of protein (n=6). **D.** Analysis of inhibitory activity of novel pyridazine derivatives (0, 0.1, 0.5, 1, 5, 10, 25, 50 and 100 nM) on Nalm6 cell-free extracts (4 μg). Fluorescence measurement showing unutilized NAD^+ and plotted as % unutilized NAD^+ over log concentration of inhibitors. **E.** Table showing IC₅₀ values for inhibition of PARP activity. The inhibition was calculated and presented with \pm SEM (n=5).

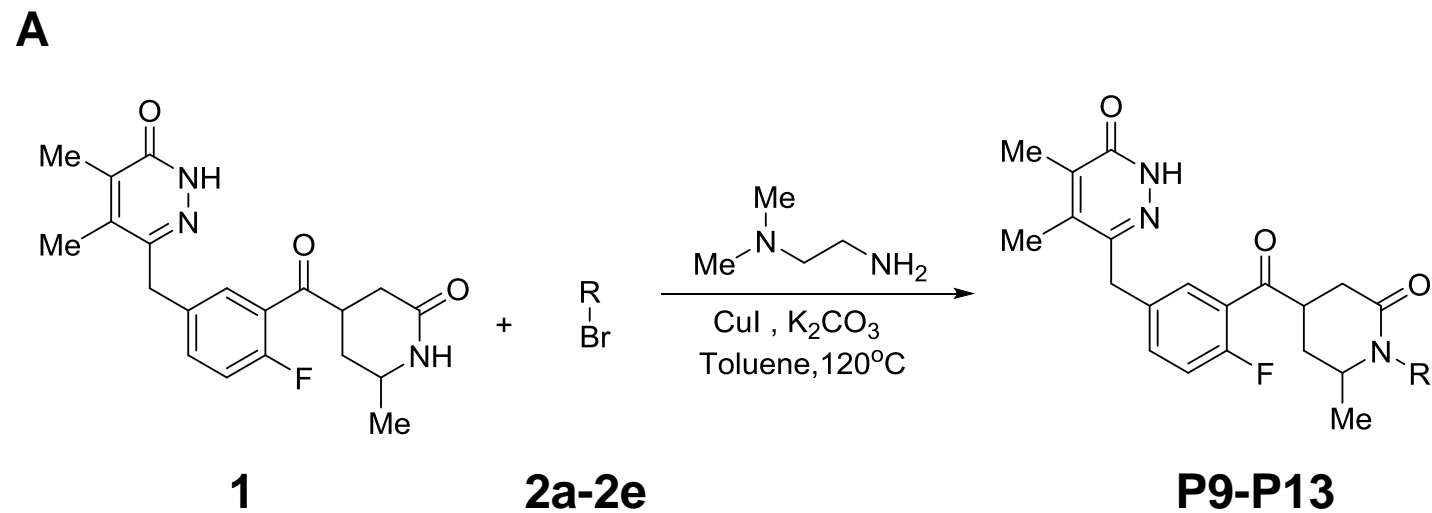
Figure 3. Evaluation of purified PARP1 enzyme inhibition by novel pyridazine derivatives. Human full length PARP1 was purified and assessed for its enzymatic inhibition in presence of pyridazine derivatives. **A.** CBB stained PAGE profile showing the purification profile of PARP1, purified using Nickel-NTA and PC11 column chromatography as described in Methods. Molecular weight ladders are indicated. **B.** Western blotting showing identity of purified PARP1 protein. **C.** PARP1 enzymatic activity in presence of different concentration of novel pyridazine derivatives (0, 0.5, 1, 5, 10, 25, 50 and 100 nM). Fluorescence measurements of unutilized NAD^+ was plotted as % unutilized NAD^+ . **D.** Table showing IC₅₀ values based on PARP1 inhibition by pyridazine derivatives. Data is presented with \pm SEM (n=6).

Figure 4. Evaluation of cytotoxicity induced by novel pyridazine derivatives in different leukemic cells. **A.** MTT assay results showing effect of novel pyridazine derivatives (0, 1, 5, 25 and 125 μM for 48 and 72 h) on proliferation of K562, Molt4, Nalm6

and REH cells. Olaparib was used as a positive control. **B.** Table showing growth inhibition (GI50) following treatment with different pyridazine derivatives on different leukemic cells.

Figure 5. Electrophoretic mobility shift assay to assess the trapping of PARP1 to DNA in presence of potential PARP1 inhibitors. **A.** Evaluation of binding of increasing concentrations of purified PARP1 (0, 5, 10, 20, 50 and 100 nM) with radiolabelled nicked DNA substrate. Schematic of the nicked DNA substrate is also shown. **B.** Bar diagram showing quantification of the unbound nicked DNA substrate following incubation with increasing concentration of PARP1 is shown and error bars indicated (n=3). **C.** Effect of NAD^+ on PARP1 binding with nicked DNA substrate. EMSA studies were carried out using PARP1 (20 nM) along with radiolabelled nicked DNA substrate in presence of different concentration of NAD^+ (0, 0.1, 1, 10, 100 and 1000 μM). **D.** Quantification showing binding of PARP1 to DNA substrate when incubated in presence of different concentration of NAD^+ and represented as bar diagram (n=3) with error bar. **E.** EMSA studies to check the trapping of PARP1 with nicked DNA in presence of newly synthesized pyridazine derivatives. PARP1 protein (20 nM) along with nicked DNA substrate was subjected to EMSA studies in presence of 1 mM NAD^+ and different concentrations of newly synthesized pyridazine derivatives (0, 0.2, 1 and 5 μM), Olaparib was used as a positive control. **F.** Bar diagram showing quantification of the PARP1 bound nicked DNA substrate, when incubated in presence of different inhibitors. Data shown are based on minimum of three independent experiments.

Figure 6. Effect of potential PARP1 inhibitors on cell cycle progression. **A.** Effect of newly synthesized pyridazine derivatives P9, P10 and P13 (10 μM , after 12, 24 and 48 h of treatment) on cell cycle progression following treatment in Nalm6 cells. Propidium iodide stained cells were analysed using flow cytometry and results were presented as histograms. DMSO treated cells were used as control. **B.** Bar diagram showing distribution of cells at different cell cycle phases G1, G2/M, S and SubG1 phase were calculated and represented as percentage with error bars (n=3).



B

Entry	Compound	R group
1	P9	2a
2	P10	2b
3	P11	2c
4	P12	2d
5	P13	2e

Figure 1

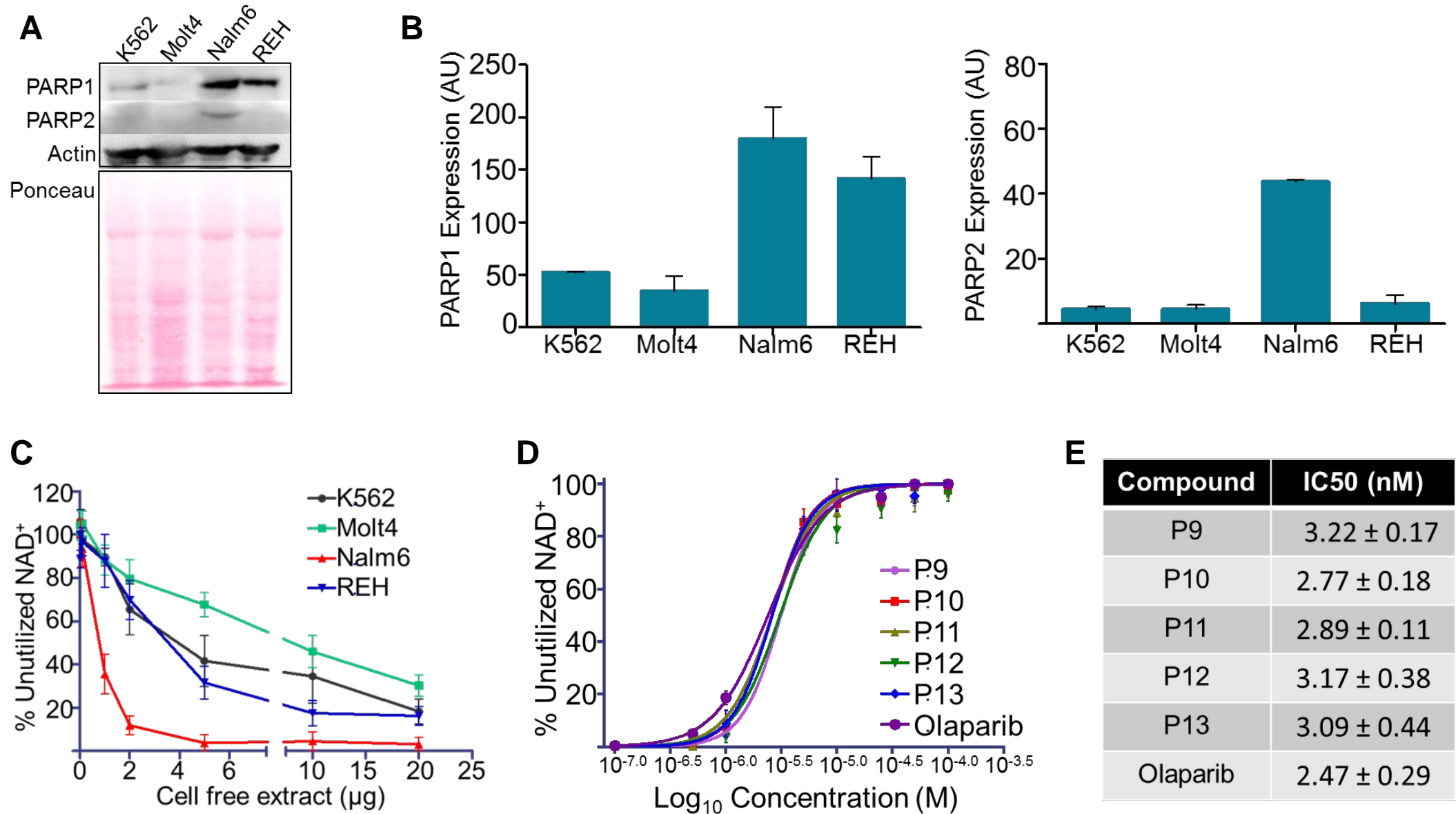
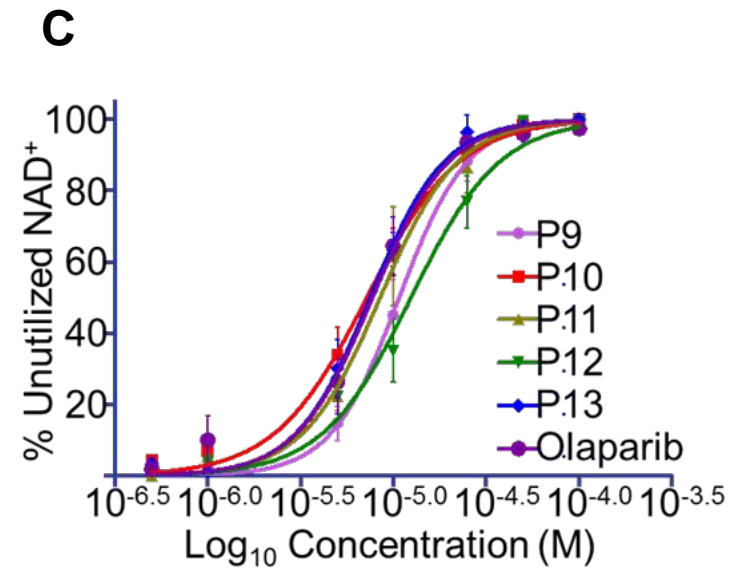
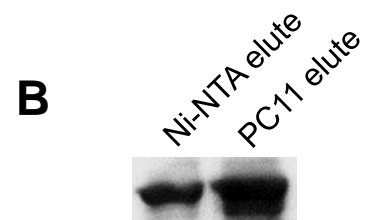
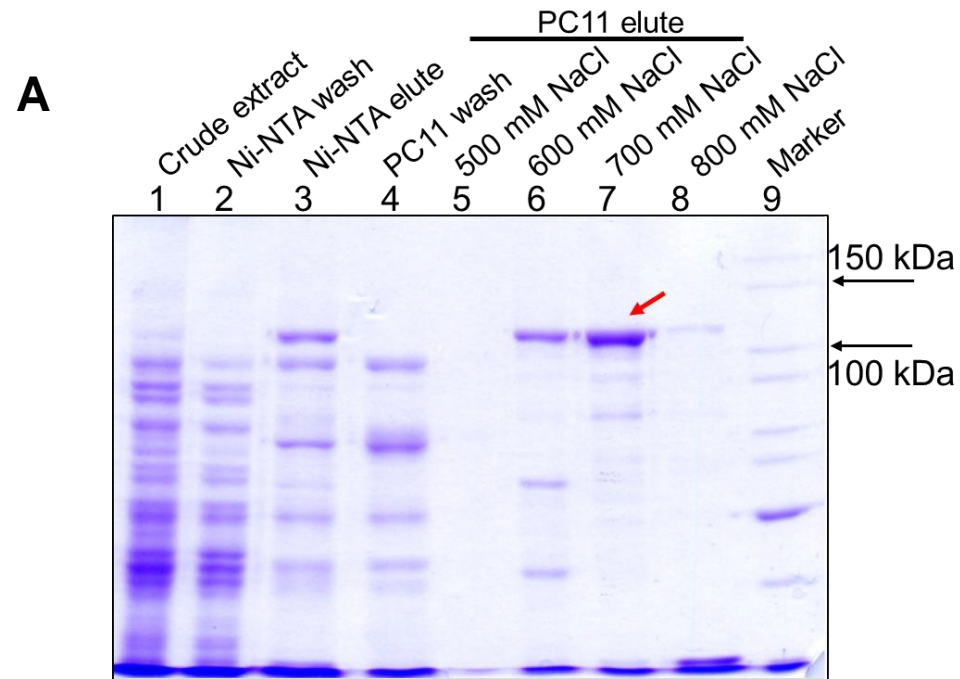


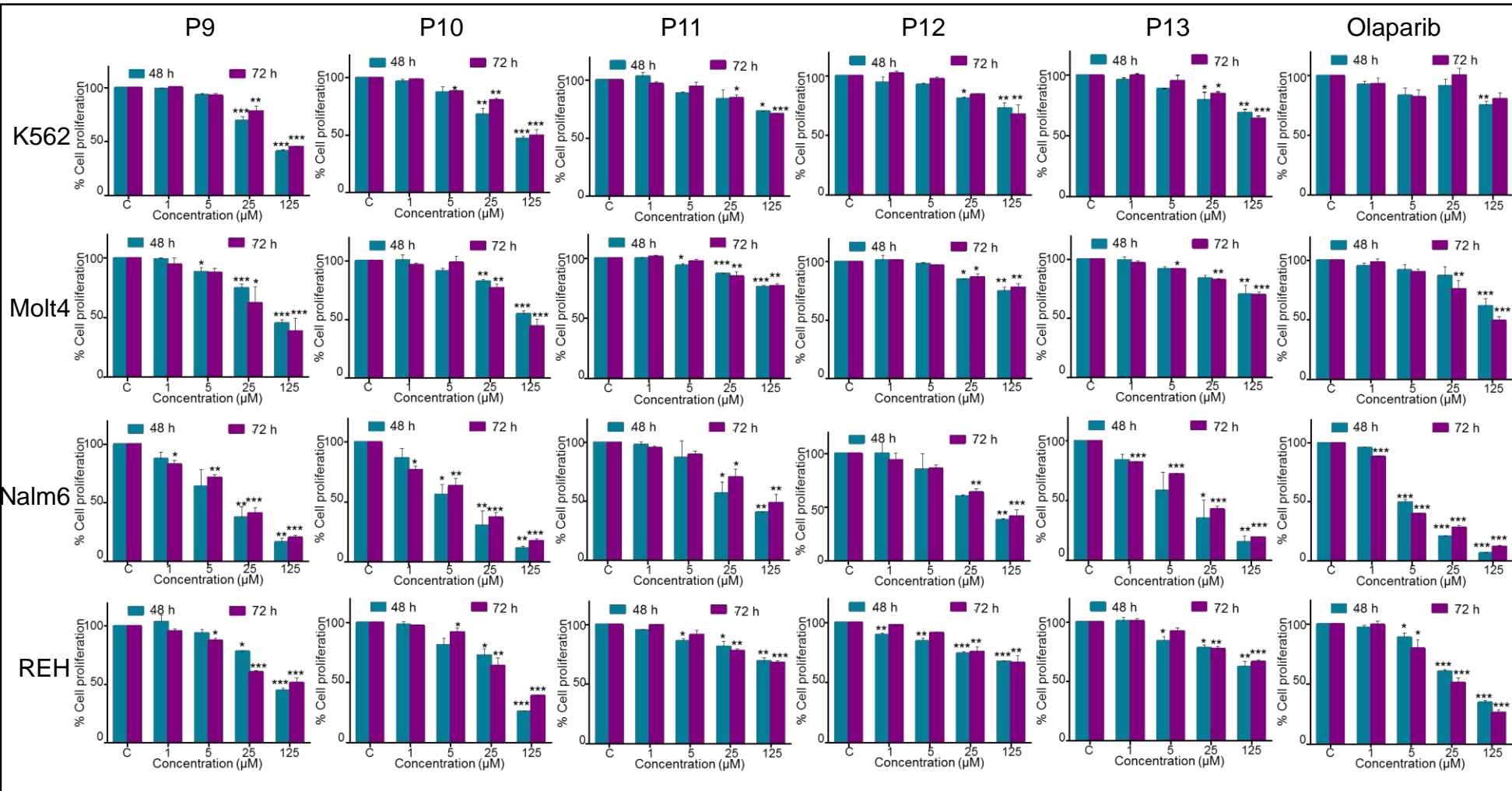
Figure 2



D

Compound	IC ₅₀ (nM)
P9	11.6 ± 1.84
P10	7.41 ± 1.2
P11	12.5 ± 2.27
P12	12.31 ± 2.79
P13	7.58 ± 0.9
Olaparib	7.8 ± 1.28

A

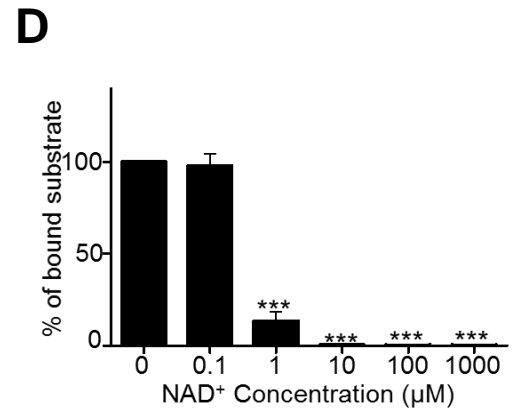
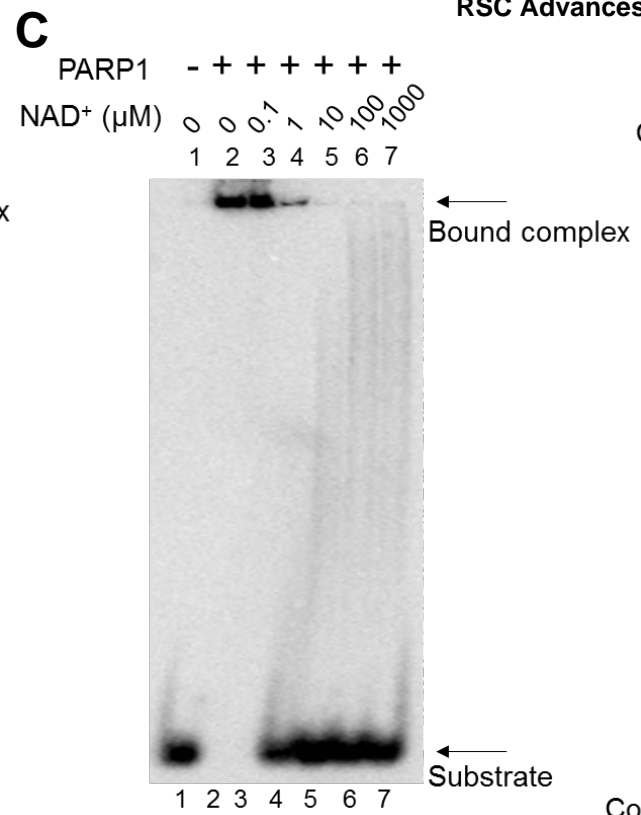
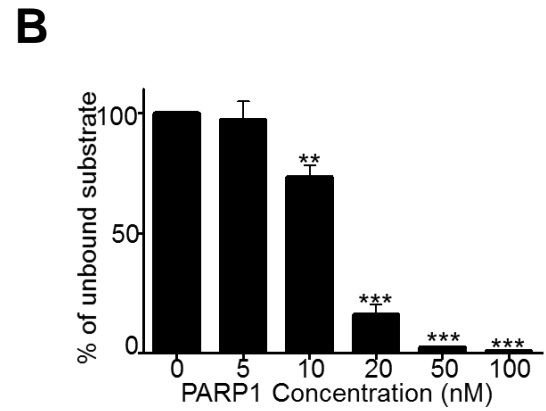
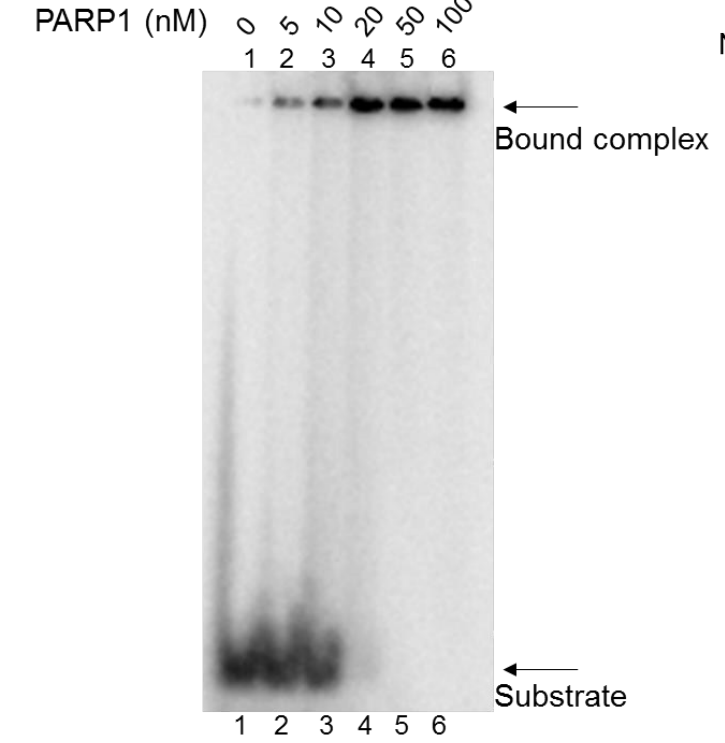
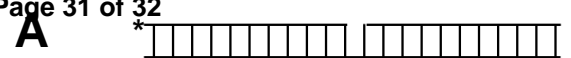


B

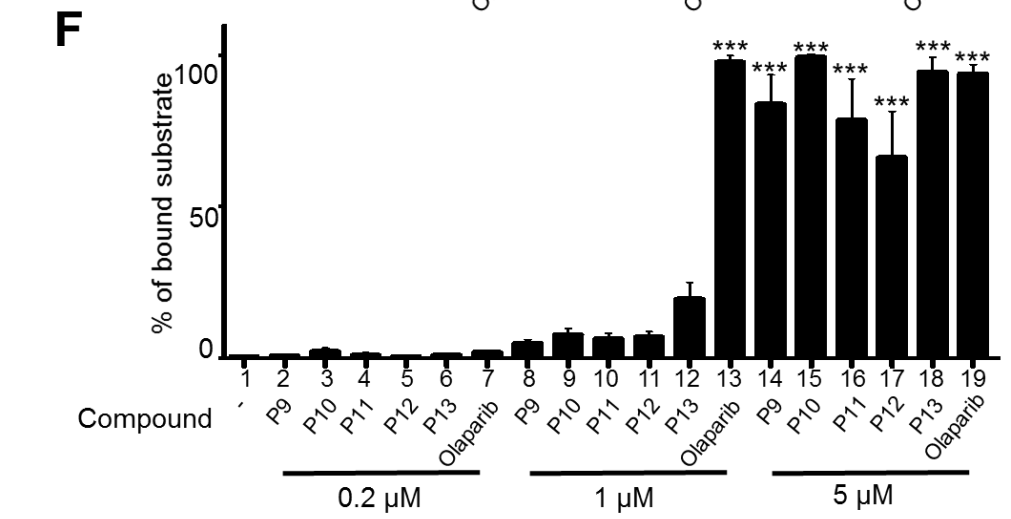
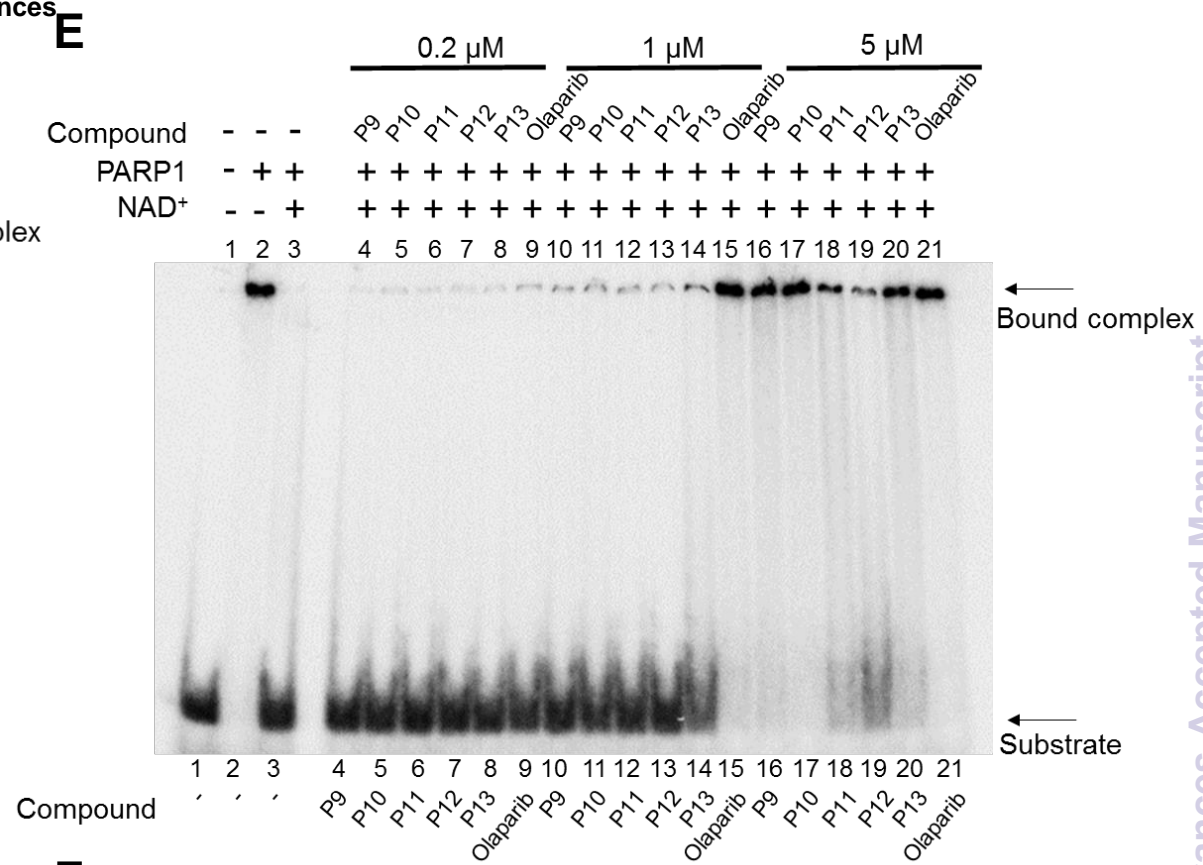
GI 50 table

Name	K562 (μM)	Molt4 (μM)	Nalm6 (μM)	REH (μM)
P9	>50	>50	12.71	>50
P10	>50	>50	8.84	~50
P11	>50	>50	~50	>50
P12	>50	>50	~50	>50
P13	>50	>50	10.33	>50
Olaparib	>50	>50	7.07	48.75

Figure 4



RSC Advances



RSC Advances Accepted Manuscript

Figure 5

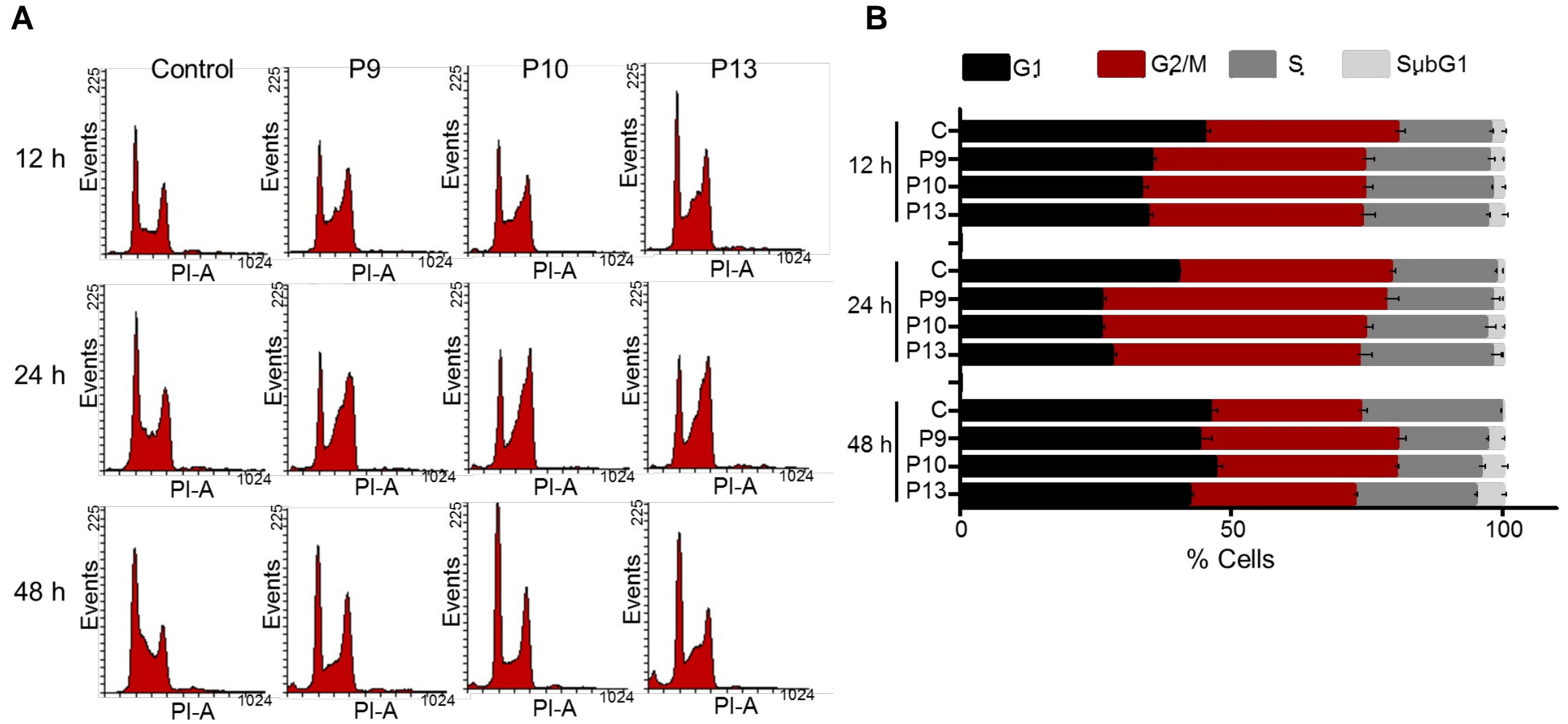


Figure 6